JOURNAL OF MOLECULAR SPECTROSCOPY 89, 421–429 (1981)

Heterodyne Frequency Measurements (at 11.6 μm) on Isotopic Species of Carbonyl Sulfide, $OC^{34}S$, $O^{13}CS$, $OC^{33}S$, ^{18}OCS, and $O^{13}C^{34}S$

J. S. WELLS AND F. R. PETERSEN

Time and Frequency Division, National Bureau of Standards, Boulder, Colorado 80303

A. G. MAKI

Molecular Spectroscopy Division, National Bureau of Standards, Washington, D. C. 20234

AND

D. J. SUKLE

Division of Science, Community College of Denver, Westminster, Colorado 80030

Heterodyne frequency measurements between a frequency-stabilized $^{13}CO_2$ reference laser and a tunable diode laser (either tuned or locked to various carbonyl sulfide absorption peaks) have been made on a number of 10^00-00^00 band transitions in the isotopic species of carbonyl sulfide: $OC^{34}S$, $O^{13}CS$, $OC^{33}S$, ^{18}OCS, and $O^{13}C^{34}S$. These OCS frequency measurements have been combined with existing microwave data and new sets of molecular constants obtained. These constants will be used later to form part of a frequency calibration compendium based on OCS.

INTRODUCTION

NBS efforts to provide improved absorption-type frequency standards for use by tunable laser users have resulted in calibration papers based on wavelength metrology on some bands of OCS (*1*) and N_2O (*2*). More recently frequency metrology techniques (or laser heterodyne experiments) and calculations (*3–6*) have been used to improve the accuracy of one of these standards, carbonyl sulfide. Because of the moderate abundance of the isotopic species of OCS, lines which do not appear in the existing OCS calibration tables can be observed and have led to some confusion. These measurements, therefore, were motivated by the need to predict the location of the isotopic lines. This paper is concerned with 4.2% abundant $OC^{34}S$, 1.1% abundant $O^{13}CS$, 0.75% abundant $OC^{33}S$, 0.2% abundant ^{18}OCS, and 0.05% abundant $O^{13}C^{34}S$.

Heterodyne frequency measurements on these isotopic species have been combined with existing microwave measurements and tunable diode laser (TDL) measurements (utilizing a Ge etalon to measure the isotopic species relative to normal OCS (*4*)) to obtain the best available constants for these isotopic species. The constants will be used to predict the frequencies of the isotopic species in a

0022-2852/81/100421-09$02.00/0

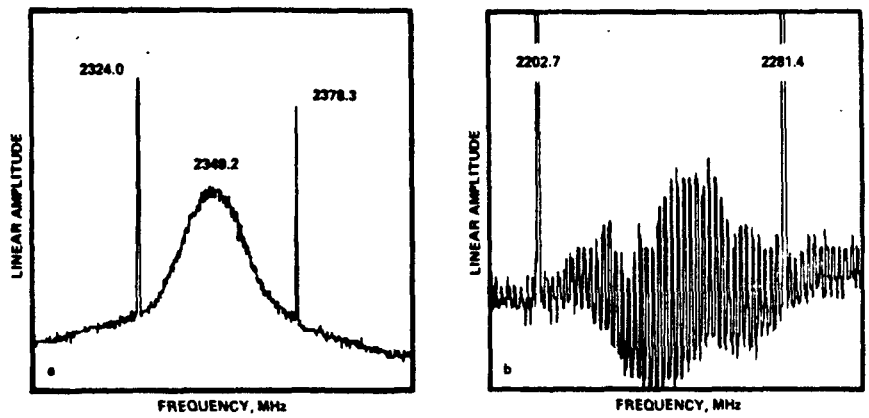

FIG. 2. (a) Signal averager recording of the beat note between the hot band line $P(25)$ of the $^{13}CO_2$ laser and TDL #2 (in helium dewar) when locked to the $R(19)$ line of $O^{13}CS$. (b) Signal averager recording of beat note between $^{13}CO_2$, $P(48)$ normal transition and TDL #2 (in closed cycle cooler) when locked to $R(63)$ of $OC^{34}S$. The shaded region produced by chopping the TDL beam defines the TDL linewidth, which has a long tail extending more than 50 MHz to the right of the 2281.4-MHz marker. Nonuniformities in the IF amplifiers and associated electronics response are also evident. Low-level beat signals required a longer averaging time which magnified the nonuniform response. (This particular measurement was not used in our fit).

TDL. A second major change is the frequency stabilization of the 2-m $^{13}CO_2$ laser (*10*) by locking it to standing-wave saturation resonances in an external CO_2 absorption cell. This stabilization scheme also permits locking to the $^{13}CO_2$ hot band (*4*, *9*) which is used as a reference for most of the frequency measurements of the isotopic OCS transitions. This stabilization apparatus was not available during the initial phase of these measurements.

The two TDLs used in these measurements had somewhat different characteristics and dictated different measurement techniques. Basically three different types of modes were observed with TDL #1, which operated best in the helium dewar. Mode A of this TDL was nearly ideal; the TDL had moderate power outputs (estimated to be about 1 μW per mode at the heterodyne detector) and a nominal 2-MHz linewidth (a 2-MHz linewidth has also been observed when this TDL was in the closed-cycle cooler). With this mode, we employed the derivative lock technique (*3*) and generally could make a measurement with a 2-MHz uncertainty. Mode B of TDL #1 typically had a narrow linewidth but such low output power at the mixer (less than 0.1 μW per mode) that the frequency modulation for the lock made the beat note virtually undetectable at OCS–$^{13}CO_2$ difference frequencies above 1200 MHz. In order to utilize this mode, we removed the lock modulation. The TDL beam was then chopped and the current sweep manually stopped at the maximum absorption indicated on the recorder trace. Our final procedure consisted of approaching the maximum absorption from both above and below to compensate for a frequency–current hysteresis and then averaging the measurements if they did not agree. Mode C of TDL #1 typically had higher power (10 μW or so) at the mixer, but unfortunately its linewidth exceeded 100 MHz.

TDL #2 operated best in the closed-cycle cooler and did not have as wide a variation in mode quality as TDL #1. Even in the helium dewar, however, the line-

TABLE I

Heterodyne Frequency Measurements of Some Absorption Lines in the 10^00-00^00 Bands of Isotopic Species of Carbonyl Sulfide at 11.6 μm.

Molecular Species	Rot. Trans.	OCS - $^{13}CO_2$ Meas. Freq. Diff. (MHz)	Measured OCS Freq. (MHz)[a]	Obs.-Calc. (MHz)	$^{13}CO_2$ Laser[b] Transition	$^{13}CO_2$ Freq.[c] (MHz)
$^{16}O^{12}C^{34}S$	R(89)	-2323.0	26 332 453.5 (4.0)	0.5	P(40)	26 334 776.5
	R(63)	+2255.4	26 098 705.9 (2.0)	-0.5	P(48)	26 096 450.5
	R(50)	-1602.6	25 972 008.2 (5.0)	0.5	P(52)	26 973 610.8
	R(44)	+ 119.5	25 911 378.9 (3.0)	1.1	P(54)	25 911 259.4
	R(38)	+ 558.0	25 849 403.1 (2.0)	-2.1	P(25)	25 848 845.1[d]
	R(35)	+2356.3	25 817 920.7 (2.0)	1.7	P(26)	25 815 564.4[d]
	R(28)	+2869.0	25 743 164.6 (3.0)	-0.3	P(29)	25 740 295.6[d]
$^{16}O^{13}C^{32}S$	R(90)	- 487.2	26 562 965.9 (5.0)	1.5	P(32)	26 563 453.1
	R(71)	- 930.3	26 391 913.7 (4.0)	-0.8	P(38)	26 392 844.0
	R(65)	+ 83.3	26 334 859.8 (6.0)	-2.3	P(40)	26 334 776.5
	R(53)	- 338.1	26 216 492.4 (3.0)	-1.7	P(44)	26 216 830.5
	R(45)	+ 899.4	26 134 476.3 (6.0)	0.5	P(14)	26 133 576.9[d]
	R(33)	- 548.5	26 006 878.0 (5.0)	3.0	P(19)	26 007 426.5[d]
	R(30)	+ 516.8	25 974 127.6 (2.0)	-0.2	P(52)	25 973 610.8
	R(19)	+2349.2	25 851 194.3 (3.0)	1.0	P(25)	25 848 845.1[d]
	R(16)	+1325.4	25 816 889.8 (4.0)	-1.3	P(26)	25 815 564.4[d]
	R(14)	-1016.0	25 793 837.4 (6.0)	-2.4	P(27)	25 794 853.4[d]
	P(2)	+1108.8	25 592 036.1 (5.0)	0.7	P(34)	25 590 927.3[d]
$^{16}O^{12}C^{33}S$	R(70)	+2223.6	26 337 000.1 (7.0)	2.3	P(40)	26 334 776.5
	R(34)	+2233.6	25 975 850.5 (6.0)	9.7	P(52)	25 973 616.9
	R(13)	+2379.2	25 742 674.8 (9.0)	-5.0	P(29)	25 740 295.6[d]
$^{16}O^{12}C^{32}S$	R(92)	+1562.4	26 036 902.3 (7.0)	-1.5	P(50)	26 035 339.9
	R(85)	+1251.4	25 978 653.6 (4.0)	1.0	P(20)	25 977 402.2[d]
	R(70)	-1036.6	25 847 808.5 (3.0)	-1.0	P(25)	25 848 845.1[d]
	R(58)	-2947.0	25 737 348.6 (2.0)	0.4	P(29)	25 740 295.6[d]
	R(43)	+1282.6	25 592 209.9 (5.0)	-0.4	P(34)	25 590 927.3[d]
$^{16}O^{13}C^{34}S$	R(85)	+ 235.1	26 157 181.4 (8.0)	2.0	P(46)	26 156 946.3
	R(54)	+1360.3	25 871 501.1 (3.0)	-1.3	P(24)	25 870 140.8[d]
	R(41)	+ 522.0	25 740 817.6 (5.0)	6.1	P(29)	25 740 295.6[d]

a The estimated uncertainty (2 σ)in MHz is given in parentheses.

b A 1.25 m stabilized $^{13}CO_2$ laser was used for lines up to P(46). For J above P(46) and for hot band transitions, a 2 m laser was used.

c Except for hot band lines, laser reference frequencies were taken from Freed, Bradley and O'Donnell [8].

d Recent NBS measurements of lasing $^{13}CO_2$ hot band transitions $[01^11 - (11^10, 03^10)_1]$.

width was about 10 MHz for TDL #2. Frequently it was wider because of frequency modulation from the derivative lock and mechanical vibration from the closed-cycle cooler. The effect of cooler vibration made it difficult (especially when working with the poorer modes) to locate the center of the beat note on the spectrum

TABLE II

Less Accurate Diode Laser Measurements on the 10^00-00^00 Transitions for Isotopically Substituted OCS

$^{16}O^{13}C^{34}S$			$^{16}O^{13}C^{32}S$			$^{16}O^{13}C^{33}S$		
Transition	Measured Frequency[a] (MHz)	O-C (MHz)	Transition	Measured Frequency[a] (MHz)	O-C (MHz)	Transition	Measured Frequency[a] (MHz)	O-C (MHz)
P(32)	25 017 498 (23)	18	P(38)	25 130 543 (30)	-1	P(44)	25 016 368 (20)	21
P(23)	25 132 777 (48)	- 4	P(21)	25 354 207 (26)	2	P(36)	25 123 597 (28)	- 1
P(5)	25 354 905 (20)	0	P(20)	25 367 068 (80)	25	P(34)	25 150 030 (40)	-30
P(4)	25 366 960 (80)	48	P(14)	25 443 314 (60)	-10	P(18)	25 356 689 (12)	1
R(1)	25 438 214 (16)	2	P(13)	25 455 914 (52)	1	P(17)	25 369 319 (16)	16
R(2)	25 449 957 (12)	-14	P(12)	25 468 464 (52)	- 3	P(11)	25 444 225 (64)	-21
R(3)	25 461 682 (12)	-13	P(11)	25 480 989 (48)	5	P(10)	25 456 616 (60)	3
R(4)	25 473 380 (30)	- 4	P(6)	25 542 962 (76)	-75	P(8)	25 481 253 (48)	14
R(5)	25 485 051 (80)	14	P(5)	25 555 349 (25)	8	R(14)	25 754 142 (76)	- 7
R(10)	25 542 719 (76)	-48	P(4)	25 567 636 (20)	28	R(15)	25 765 564 (20)	-18
R(11)	25 554 231 (16)	25	P(2)	25 592 032 (16)	- 3	R(16)	25 776 962 (16)	-16
R(12)	25 565 627 (12)	17	P(1)	25 604 192 (12)	- 3	R(17)	25 788 327 (12)	-11
R(13)	25 576 990 (50)	13	R(11)	25 758 998 (36)	9	R(18)	25 799 644 (20)	-17
R(15)	25 599 605 (28)	0	R(12)	25 770 621 (40)	-21	R(21)	25 833 401 (12)	-11
R(29)	25 753 965 (80)	11	R(13)	25 782 250 (50)	- 9	R(25)	25 877 938 (60)	37
R(30)	25 764 703 (12)	- 3	R(14)	25 793 837 (48)	- 3	R(43)	26 070 759 (36)	- 3
R(32)	25 786 103 (12)	1	R(15)	25 805 379 (48)	- 5	R(44)	26 081 125 (36)	4
R(33)	25 796 748 (24)	4	R(18)	25 839 801 (40)	5	R(61)	26 251 363 (20)	-24
R(34)	25 807 355 (50)	5	R(21)	25 873 882 (24)	4			
R(37)	25 838 977 (32)	30	R(22)	25 885 208 (20)	43			
R(41)	25 880 561 (16)	2	R(31)	25 985 087 (12)	6			
R(51)	25 981 990 (40)	9	R(37)	26 050 007 (36)	- 6			
R(58)	26 050 735 (32)	- 2	R(38)	26 060 707 (40)	4			
R(59)	26 060 398 (44)	-10	R(39)	26 071 352 (40)	- 4			
R(60)	26 070 036 (36)	- 4	R(40)	26 081 974 (30)	3			
R(61)	26 079 641 (24)	7	R(55)	26 236 610 (24)	- 3			
			R(56)	26 246 608 (30)	- 6			
			R(57)	26 256 576 (32)	0			
			R(58)	26 266 481 (36)	-18			
			R(59)	26 276 377 (44)	- 6			
			R(60)	26 286 240 (44)	12			
			R(61)	26 296 029 (52)	- 5			
			R(62)	26 305 811 (55)	11			
			R(63)	26 315 527 (28)	0			

$^{18}O^{13}C^{34}S$		
Transition	Measured Frequency[a] (MHz)	O-C (MHz)
P(12)	25 132 240 (44)	- 4
R(6)	25 358 218 (12)	1
R(13)	25 438 256 (16)	- 3
R(14)	25 449 544 (12)	- 7
R(15)	25 460 804 (16)	- 4
R(16)	25 472 019 (50)	-10
R(23)	25 549 578 (24)	7
R(24)	25 560 545 (40)	41
R(27)	25 593 090 (24)	2
R(42)	25 751 105 (80)	17
R(43)	25 761 334 (16)	7
R(44)	25 771 533 (40)	4
R(47)	25 801 914 (20)	1
R(48)	25 811 978 (20)	11
R(50)	25 831 947 (28)	-15
R(54)	25 871 499 (12)	- 3
R(55)	25 881 278 (12)	-15

a) The estimated uncertainty (2 σ) in MHz is given in parentheses.

analyzer and prompted the use of the signal averager indicated in Fig. 1. Frequency markers were superposed on either side of the beat note and the beat note center could be determined at a later time from a recording of the averaged signal. One of the better averaged displays is shown in Fig. 2a. The signal averager was particularly useful in a frequency region 400 MHz wide and centered at 2200 MHz, where the frequency response of the IF amplifiers and other electronics was highly nonuniform. By chopping the TDL beam at a rate related to the sweep rate one can readily distinguish the TDL lineshape from various nonuniformities in response which are manifest as baseline irregularities. The chopper produced the display in Fig. 2b. Some of the features exhibited there, i.e., broad and asymmetric

TABLE IV

Variance–Covariance Matrix Elements (MHz^2) for the 10^00-00^00 Bands of $OC^{34}S$, $O^{13}CS$, $OC^{33}S$, ^{18}OCS, and $O^{13}C^{34}S$

$^{16}O^{12}C^{34}S$	ν_0	B'	D'	B"	D"
ν_0	2.08479	-1.19826×10^{-3}	-1.23814×10^{-7}	1.04964×10^{-6}	6.37099×10^{-10}
B'		8.87211×10^{-7}	1.13571×10^{-10}	7.49830×10^{-9}	1.33384×10^{-11}
D'			4.17637×10^{-14}	1.04723×10^{-11}	2.98187×10^{-14}
B"				7.43859×10^{-9}	1.09250×10^{-11}
D"					3.08602×10^{-14}
$^{16}O^{13}C^{32}S$					
ν_0	1.48451	-7.97878×10^{-4}	-7.63670×10^{-8}	4.04603×10^{-6}	4.08076×10^{-9}
B'		8.92399×10^{-7}	1.33504×10^{-10}	1.52112×10^{-8}	2.62621×10^{-11}
D'			8.00613×10^{-14}	2.34357×10^{-11}	5.69882×10^{-14}
B"				1.80982×10^{-8}	2.48527×10^{-11}
D"					6.98591×10^{-14}
$^{16}O^{12}C^{33}S$					
ν_0	5.97162	4.74564×10^{-5}	2.83775×10^{-8}	-4.40601×10^{-6}	-2.74535×10^{-9}
B'		9.12537×10^{-8}	3.26905×10^{-11}	5.39219×10^{-10}	2.53201×10^{-13}
D'			1.35744×10^{-14}	2.51784×10^{-13}	1.18453×10^{-16}
B"				1.05306×10^{-8}	3.81340×10^{-12}
D"					1.59163×10^{-15}
$^{18}O^{12}C^{32}S$					
ν_0	7.66447	-1.94210×10^{-3}	-1.03537×10^{-7}	1.35310×10^{-5}	3.63331×10^{-9}
B'		8.96698×10^{-7}	9.12018×10^{-11}	6.19909×10^{-9}	2.44948×10^{-12}
D'			1.38352×10^{-14}	3.29449×10^{-12}	1.32337×10^{-15}
B"				1.18941×10^{-8}	3.96011×10^{-12}
D"					1.51857×10^{-15}
$^{16}O^{13}C^{34}S$					
ν_0	12.9454	-6.38404×10^{-3}	-6.28181×10^{-7}	4.36759×10^{-6}	1.64298×10^{-9}
B'		4.01219×10^{-6}	4.62497×10^{-10}	1.29394×10^{-8}	4.89287×10^{-12}
D'			6.43772×10^{-14}	5.36084×10^{-12}	2.31211×10^{-15}
B"				1.57297×10^{-8}	5.90491×10^{-12}
D"					2.52569×10^{-15}

4), particularly in the case of nonenriched species ($OC^{33}S$ and $O^{13}C^{34}S$), where the absorption lines were quite weak.

DISCUSSION AND RESULTS

Since only $\Sigma-\Sigma$ transitions were measured ($l = 0$ states), the data were fitted to the equations

$$\nu_{\text{obs}} = \nu_0 + F'(J') - F''(J'') \tag{1}$$

and

$$F_v(J) = B_vJ(J + 1) - D_vJ^2(J + 1)^2. \tag{2}$$

For the microwave transitions of course, $\nu_0 = 0$, $B'_v = B''_v$, and $D'_v = D''_v$. Higher-order H terms were used in preliminary calculations but were not used in the final analysis, since the data were fitted equally well when these terms were

3. J. S. WELLS, F. R. PETERSEN, AND A. G. MAKI, *Appl. Opt.* **18**, 3567–3573 (1979).
4. J. S. WELLS, F. R. PETERSEN, A. G. MAKI, AND D. J. SUKLE, *Appl. Opt.* **20**, 1676–1684 (1981).
5. J. P. SATTLER, T. L. WORCHESKY, A. G. MAKI, AND W. J. LAFFERTY, *J. Mol. Spectrosc.*, in press.
6. A. FAYT, University of Louvain, Louvain-la-Neuve, Belgium, private communication.
7. A. G. MAKI *et al.*, *J. Phys. Chem. Ref. Data*, in press.
8. C. FREED, L. C. BRADLEY, AND R. G. O'DONNELL, *IEEE. J. Quant. Elec.* **16**, 1195–1206 (1980).
9. F. R. PETERSEN, J. S. WELLS, A. G. MAKI, AND K. SIEMSEN, *Appl. Opt.*, in press.
10. C. FREED AND A. JAVAN, *Phys. Lett.* **17**, 53–56 (1970).
11. A. G. MAKI, *J. Phys. Chem. Ref. Data* **3**, 221–244 (1974).
12. N. W. LARSEN AND B. P. WINNEWISSER, *Z. Naturforsch.* **29a**, 1213–1215 (1974).
13. J. G. SMITH, *J. Chem. Soc. Faraday Trans. II* **72**, 2298–2300 (1976).
14. A. DUBRULLE, J. DEMAISON, J. BURIE, AND D. BOUCHER, *Z. Naturforsch.* **35a**, 471–474 (1980).
15. A. V. BURENIN, E. N. KARYAKIN, A. F. KRUPNOV, S. M. SHAPIN, AND A. N. VAL'DOV, *J. Mol. Spectrosc.* **85**, 1–7 (1981).
16. A. V. BURENIN, A. N. VAL'DOV, E. N. KARYAKIN, A. F. KRUPNOV, AND S. M. SHAPIN, *J. Mol. Spectrosc.* **87**, 312–315 (1981).